DOI: 10.24850/j-tyca-2022-03-08

Articles

Satellite-assisted irrigation using the FAO-56 dual method: Scope and limitations

Asistencia satelital en riego usando el método dual de FAO-56: alcances y limitaciones

Fernando Paz-Pellat[1], ORCID: https://orcid.org/0000-0002-6697-2238

Martín Alejandro Bolaños-González[2], ORCID: https://orcid.org/0000-0002-8110-1051

[1]GRENASER, Colegio de Postgraduados, Campus Montecillo, State of Mexico, ferpazpel@gmail.com

[2]Posgrado en Hidrociencias, Colegio de Postgraduados, Campus Montecillo, State of Mexico, Mexico, bolanos@colpos.mx

Corresponding author: Martín Alejandro Bolaños-González, bolanos@colpos.mx

Abstract

The estimation of water requirements of crops using the FAO-56 dual method needs a robust and reliable parameterization of the crop coefficient (K_c). The use of remote sensing through vegetation indices (VI) to define a relationship with K_c is a task that requires an understanding of the scope and limitations of each. This paper sets the perspective about estimates based on VI relative to those based on K_c, noting that the latter is rather limited for not considering soil water content. Using the KIMO SAVI index and its application to two experiments (maize and wheat) with evapotranspiration measurements using lysimeters, the relationship of this index with K_c is analyzed aiming to establish a methodology for a solid parametrization of the relationships between these two approaches, using the beginning and end of the crop development stages with an expo-linear growth model. The relationships obtained in this parameterization yielded a good fit (R^2 >0.96).

Keywords: KIMO SAVI, equivalent radiative media, corn and wheat, crop coefficient.

Resumen

La estimación de los requerimientos de agua de los cultivos usando el método dual de FAO-56 necesita de la parametrización del coeficiente del cultivo (K_c) en forma robusta y confiable. El uso de sensores remotos, a través de índices de vegetación (IV), para definir una relación con K_c es una tarea que debe ser entendida en función de sus alcances y

limitaciones. En este trabajo se pone en perspectiva qué es lo que estiman los IV en relación con los K_c definiendo que su uso está limitado a no considerar el efecto de la humedad del suelo en estos últimos. Usando el índice IV_CIMAS y su aplicación a dos experimentos (maíz y trigo) con mediciones de evapotranspiración en lisímetro se analizan las relaciones de índice con K_c, a fin de establecer una metodología para parametrizar sus relaciones en forma sólida, usando los inicios y finales de las etapas de desarrollo de los cultivos por medio de un modelo expo-lineal del crecimiento. Las relaciones obtenidas en la parametrización resultaron en buenos ajustes ($R^2 > 0.96$).

Palabras clave: KIMO SAVI, medio radiativo equivalente, maíz y trigo, coeficiente de cultivo.

Received: 05/08/2020

Accepted: 04/05/2021

Introduction

Satellite-assisted irrigation involving the use of friendly products is one of the current challenges that is raising attention to the applications of remote sensing technology (Calera, Jochum, Cuesta, Montoro, & Fuster, 2005). The issues associated with satellite estimates of crop evapotranspiration (ET_c) to define the water requirements of crops need pragmatic approaches supported by sound science and experimental evidence.

Remote sensing technology allows the monitoring of vegetation growth and development through theoretical or empirical relationships between crop biophysical variables and vegetation spectral indices (VI), which are broadly available (Verstraete & Pinty, 1996; Paz *et al*., 2015). The vast majority of VI are based on the high contrast between red (R) and near-infrared (NIR) bands for vegetation (Tucker, 1979). Vegetation indices are influenced by multiple factors, including atmospheric effects, sun-sensor geometry, and the soil-vegetation mixture. In particular, the effect of soil (vegetation background) is relevant for estimating biophysical variables as well as the crop coefficient. Different VI that minimizes the effect of soil has been used, such as *GESAVI* (Gilabert, González-Piqueras, García-Haro, & Meliá, 2002) and $NDVI_{cp}$ (Paz *et al*., 2007), whose validity interval is limited to a first exponential phase of the spectral patterns associated with vegetation growth (*LAI* isolines). Romero *et al*. (2009) have developed a generalized $NDVI_{cp}$ for the exponential and linear phases (up to the peak *LAI*) using the KIMO SAVI index.

The evapotranspiration of a given crop (ET_c) is calculated by multiplying reference evapotranspiration (grass or alfalfa) by a crop coefficient ($K_c = ET_c / ET_o$). The reference evapotranspiration has been standardized to a virtual crop with predefined biophysical and aerodynamic characteristics (Allen, Pereira, Raes, & Smith, 1998).

Based on the assumption that temporary variations of VIs reflect the temporal patterns of crop coefficients (Jackson, Pinter, Reginato, & Idso,1980), the use of VI has been proposed to estimate K_c (Heilman, Heilman, & Moore, 1982). Hence, linear relationships have been proposed between K_c and several VI (Bausch & Neale, 1987; Bausch & Neale, 1989; Bausch, 1993; Bausch 1995), for use in irrigation planning.

Within a general context and from a water efficiency perspective, characterizing the exchange of matter and energy between the atmosphere and vegetation requires estimates of the leaf area index (*LAI*), height (*h*), and fractional vegetation cover (*fv*). This is true for both the use of transfer models from two or more sources (Shuttleworth & Wallace, 1985; Choudhury & Monteith, 1988), and operational energy-balance approaches such as SEBAL (Surface Energy Balance Algorithm for Land (Bastiaanssen, Menenti, Feddes, & Holtslag, 1998) and METRIC (Mapping evapotranspiration at high resolution and with internalized calibration (Allen, Tasumi, & Trezza, 2005), including the simplified methods proposed by FAO (Allen *et al*., 1998).

This paper analyzes the scope and limitations of the methodology involving the use of VIs to estimate crop coefficients and introduces an operational approach for the use of optimized VI in K_c estimates.

Theory

Spectral Vegetation Indices, Biophysical Variables, and K_c

The analysis of patterns associated with spectral vegetation indices (VI) warrants a reference theoretical framework that allows checking for consistency relative to the vegetation radiative transfer theory. This analysis format avoids using empirical considerations to define the best VI.

Figure 1a shows the temporal crop-growth pattern within the R-NIR spectral space, represented by leaf area index (*LAI*) isolines sharing the same amount of vegetation, for optically different soils; this was generated using six soil types (S2, S5, S7, S9, S11, and S12; dark-to-

Tecnología y ciencias del agua, ISSN 2007-2422, 13(3), 374-424. DOI: 10.24850/j-tyca-2022-03-08

light color gradient). Paz, Palacios, Mejía, Martínez and Palacios (2005) detail the radiative simulations shown in Figure 1a. Figure 1b depicts the outcome of an experiment with maize using sliding soil trays under the crop to simulate different optical properties of soil (Bausch, 1993).

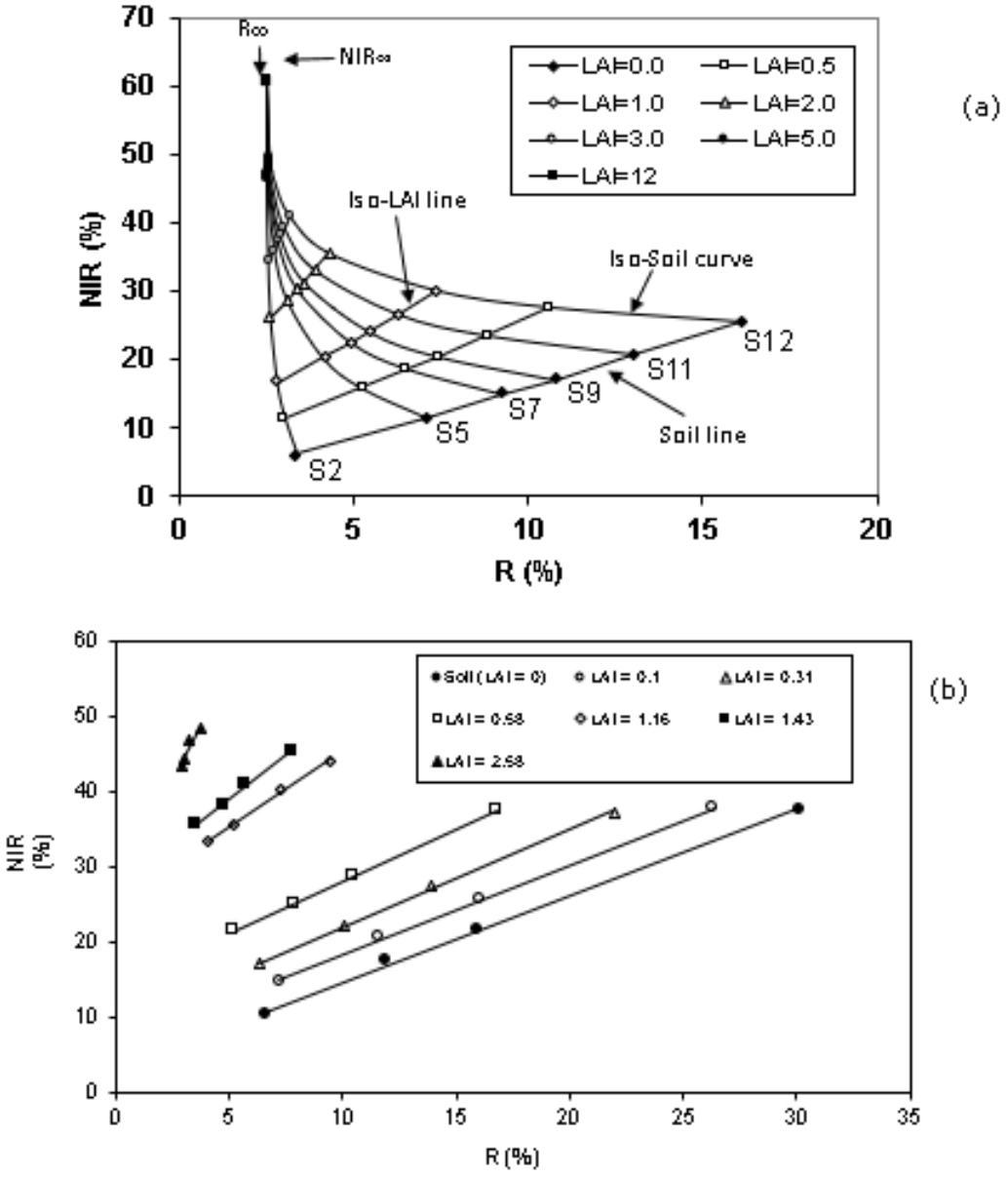

Figure 1. Spectral patterns in the R-NIR space. (a) radiative simulations, and (b) maize experiment.

Tecnología y ciencias del agua, ISSN 2007-2422, 13(3), 374-424. DOI: 10.24850/j-tyca-2022-03-08

In Figure 1, straight lines (first-order radiative interactions) were fitted to *LAI* isoline values of vegetation reflectance with variable soil reflectances (soil line in Figure 1). Figure 1 defines several important patterns to understand the behavior of both reflectance and VI during crop development: a) if points of identical leaf area index (*LAI* isolines) corresponding to each same-soil curve (soil isolines) are joined, a quasi-linear pattern emerges. Thus, the growth stage of a crop (*LAI*) produces a straight line regardless of the background soil type in the crop; b) the slope (b_0) and intercept (a_0) of *LAI* isolines vary with *LAI*. The slope of *LAI* isolines originates from a slope equal to that of the soil line (*LAI* = 0) and increases in a counter-clockwise direction to reach an angle of 90°. This latter condition corresponds to the saturation of reflectance in the R-band, represented in Figure 1 as reflectance values above the peak of the "tasseled cap" (*LAI* > 5); c) all soil isolines converge at the saturation point of visible bands. Convergence approaches a straight line (apex in Figure 1); the R-band reaches a saturation point, but the *NIR* continues growing to its saturation point. The saturation points also called infinite reflectance ($R\infty$ or $NIR\infty$) or dense medium, is a function of the optical properties of leaves and their angular distribution (Ross, 1981).

Figure 2a, the case of radiative simulations, shows the relationship between a_0 and b_0 of *LAI* isolines for the crop-growth cycle ranging from bare soil to 100 % vegetation coverage. The early-stage shows an exponential pattern up to the R-band apparent saturation point; the

Tecnología y ciencias del agua, ISSN 2007-2422, 13(3), 374-424. DOI: 10.24850/j-tyca-2022-03-08

pattern becomes linear thereafter. The starting point of the a_0-b_0 curve represents bare soil ($a_0 = a_S$; $b_0 = b_s$). The point where a_0 reaches its peak value (shift from exponential to linear) represents the end of the exponential growth phase of vegetation and the beginning of the linear vegetative growth phase (Paz, Casiano, Zarco, & Bolaños, 2013). The endpoint of the linear pattern of the a_0-b_0 curve represents the point where the NIR band may or may not become saturated, which occurs when *LAI* reaches its peak value.

Tecnología y ciencias del agua, ISSN 2007-2422, 13(3), 374-424. DOI: 10.24850/j-tyca-2022-03-08

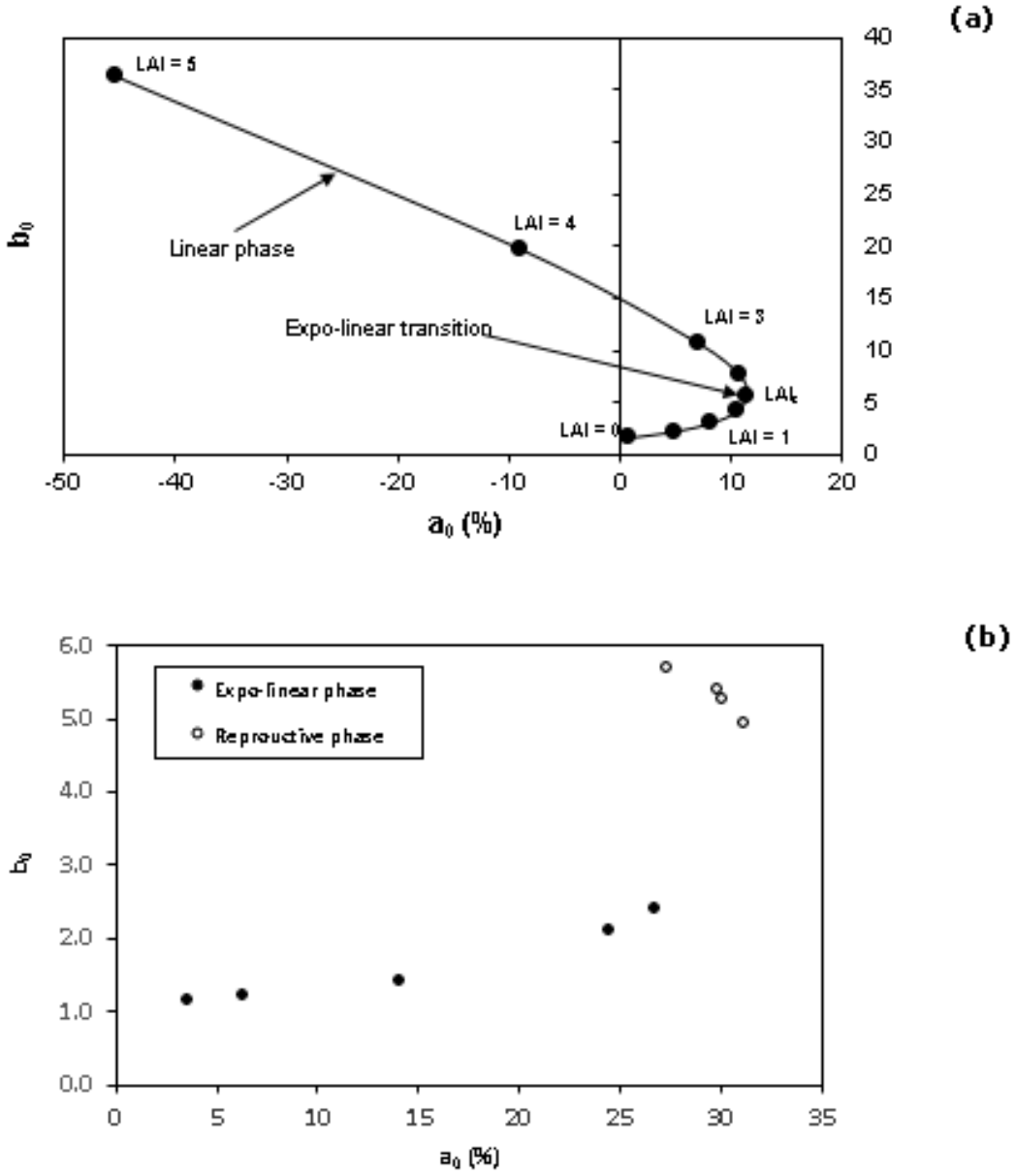

Figure 2. Patterns for parameters a_0 and b_0 of *LAI* isolines: a) radiative simulations, and b) maize experiment.

Tecnología y ciencias del agua, ISSN 2007-2422, 13(3), 374-424. DOI: 10.24850/j-tyca-2022-03-08

In Figure 2b, experimental maize data, the pattern between a_0 and b_0 is similar to that of radiative simulations, but with major differences according to the growth stages of the crop.

In the case of radiative simulations, the turbid medium approximation (Ross, 1981) assumes a homogeneous and complete soil coverage by vegetation; also, is adopted the hypothesis that the optical and geometric properties of leaves remain unchanged during crop growth (increase in *LAI*). Under these considerations, the temporal *LAI* pattern can be modeled with an expo-linear function that smoothes the exponential-to-linear shift (Goudriaan & Monteith, 1990) (Figure 3a). Figure 2a shows that the expo-linear phase has a similar pattern in the a_0-b_0 space. The expo-linear model for the variable V as a function of time t is defined according to:

$$V(t) = \frac{C}{r} ln\{1 + exp[r(t - t_b)]\} \quad (1)$$

With the following characteristics:

$$V(t = t_T) = \frac{C}{r}\ ; t_T = t_b + \frac{0.541}{r} \quad (2)$$

Tecnología y ciencias del agua, ISSN 2007-2422, 13(3), 374-424. DOI: 10.24850/j-tyca-2022-03-08

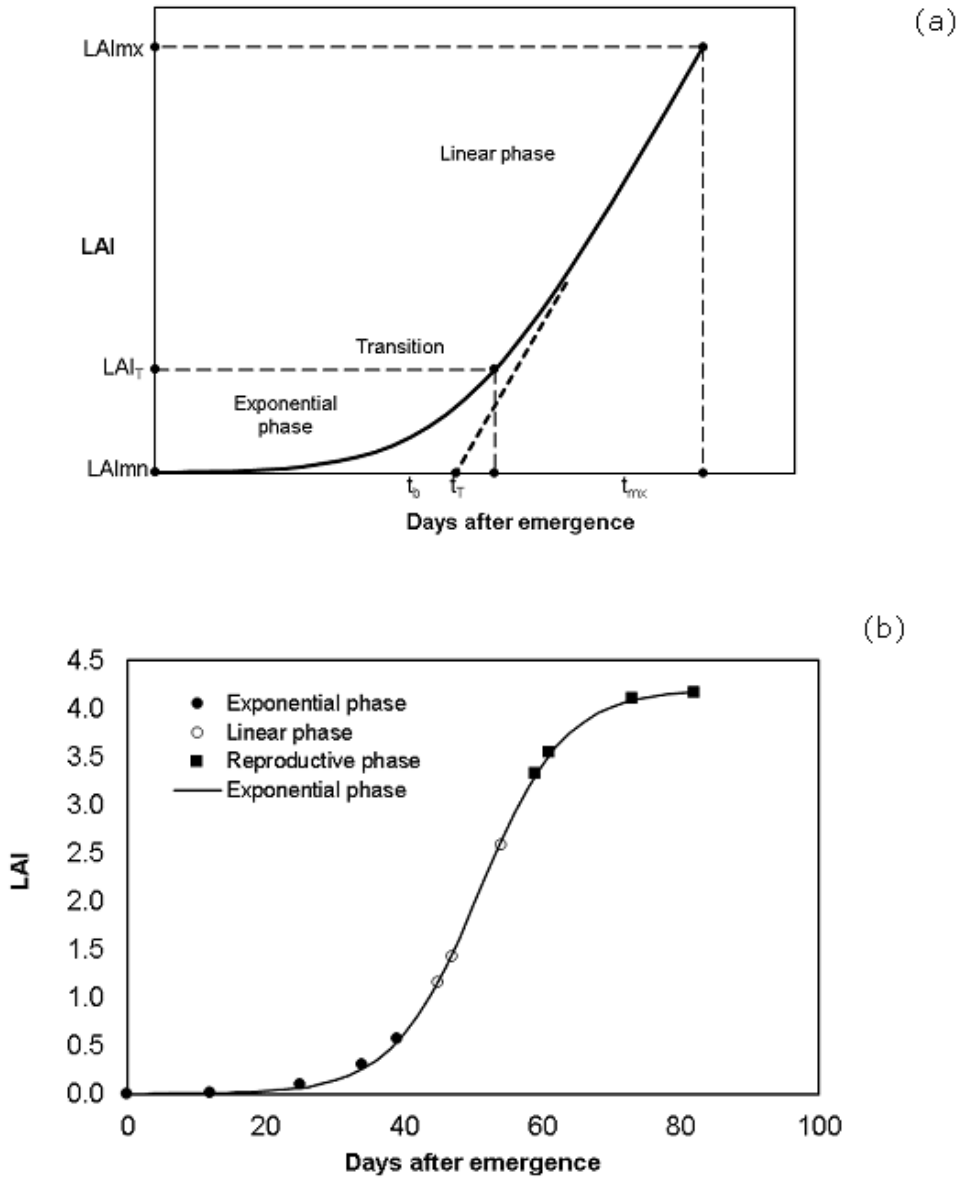

Figure 3. Temporal *LAI* patterns: a) schematic model, and b) maize experiment.

Tecnología y ciencias del agua, ISSN 2007-2422, 13(3), 374-424. DOI: 10.24850/j-tyca-2022-03-08

In the expo-linear model, Figure 3a, the transition point (shift) between the exponential and linear (*LAI*) phase occurs at time t_T. The linear phase projected to intersect the time axis, Figure 3a, is defined by the "lost time", t_b. This is the time lost (lagged) during the exponential phase until the maximum growth rate is achieved, which is maintained during the linear phase; t_{mx} is associated with the peak *LAI* in the linear phase, LAI_{mx} (which is not the peak *LAI* for the whole vegetative phase).

The expo-linear model is based on biophysical characteristics for *LAI* (an approximation to a homogeneous medium in physical terms, and to a turbid medium in radiative terms) (Ferrandino, 1989). This model has been successfully applied to the analysis of the temporal variation of vegetation indices (Odi, Paz, & Bolaños, 2010; Reyes *et al*., 2011).

For the experimental maize data, the linear pattern of a_0-b_0 in Figure 2b represents the reproductive phase, showing changes in the optical (mixture of leaves and reproductive organs) or geometric properties of leaves (angular distribution of leaves and reproductive organs). Figure 3b depicts the temporal pattern of the *LAI*, where a reproductive phase occurs after the expo-linear phase and before reaching the peak *LAI* (LAI_{mx}).

Considering the phases of crops in the vegetative growth phase, the differences between the patterns in Figure 2 are essential to understanding the errors associated with radiative models and designing generalized vegetation indices.

The core issue regarding the R-NIR space is that it induces a shift of slope in the a_0-b_0 curve, interpreted by many VI as a "saturation" of bands. In reality, there is no such saturation; this shift merely results from the fact that the linear patterns of some indices increasingly deviate from the near-linear values of the segment associated with a_0-b_0 when *LAI* is higher than 2-3. This saturation is a consequence of the format of ratios used for most VI with linear patterns in the a_0-b_0 parametric space.

Vegetation Spectral Indices

One of the most extensively used vegetation spectral indices is the normalized difference vegetation index (*NDVI*), defined as (Rouse, Haas, Schell, Deering, & Harlan, 1974):

$$NDVI = \frac{NIR-R}{NIR+R} \quad (3)$$

implying a relationship in the a_0-b_0 space of $a_0 = 0$ and $b_0 = f(NDVI)$ (Paz *et al*., 2015); that is, it assumes that all *LAI* isolines originate in (0, 0) in the R-NIR space, so that the a_0-b_0 space in Figure 2 represents a vertical

Tecnología y ciencias del agua, ISSN 2007-2422, 13(3), 374-424. DOI: 10.24850/j-tyca-2022-03-08

straight line on the b_0 axis (Paz *et al*., 2015). From Figure 1 and Figure 2, it is clear that this hypothesis is incorrect for radiative simulations as well as for experimental data.

To avoid the *NDVI* hypotheses, Paz *et al*. (2007) designed an VI that takes into account the changes in the slope b_0 according to a_0:

$$NDVIcp = \frac{b_0 - 1}{b_0 + 1} \; ; \; \frac{1}{b_0} = c + d a_0 \qquad (4)$$

where *c* and *d* are two empirical constants associated with the pattern in Figure 2b.

Figure 4 shows the results of applying *NDVI* and $NDVI_{cp}$ to the maize experiment (four background soils with different optical properties) in Figure 1b. Besides the variations in *NDVI* values for different soils, this becomes saturated at an *LAI* of around 2, unlike $NDVI_{cp}$.

Tecnología y ciencias del agua, ISSN 2007-2422, 13(3), 374-424. DOI: 10.24850/j-tyca-2022-03-08

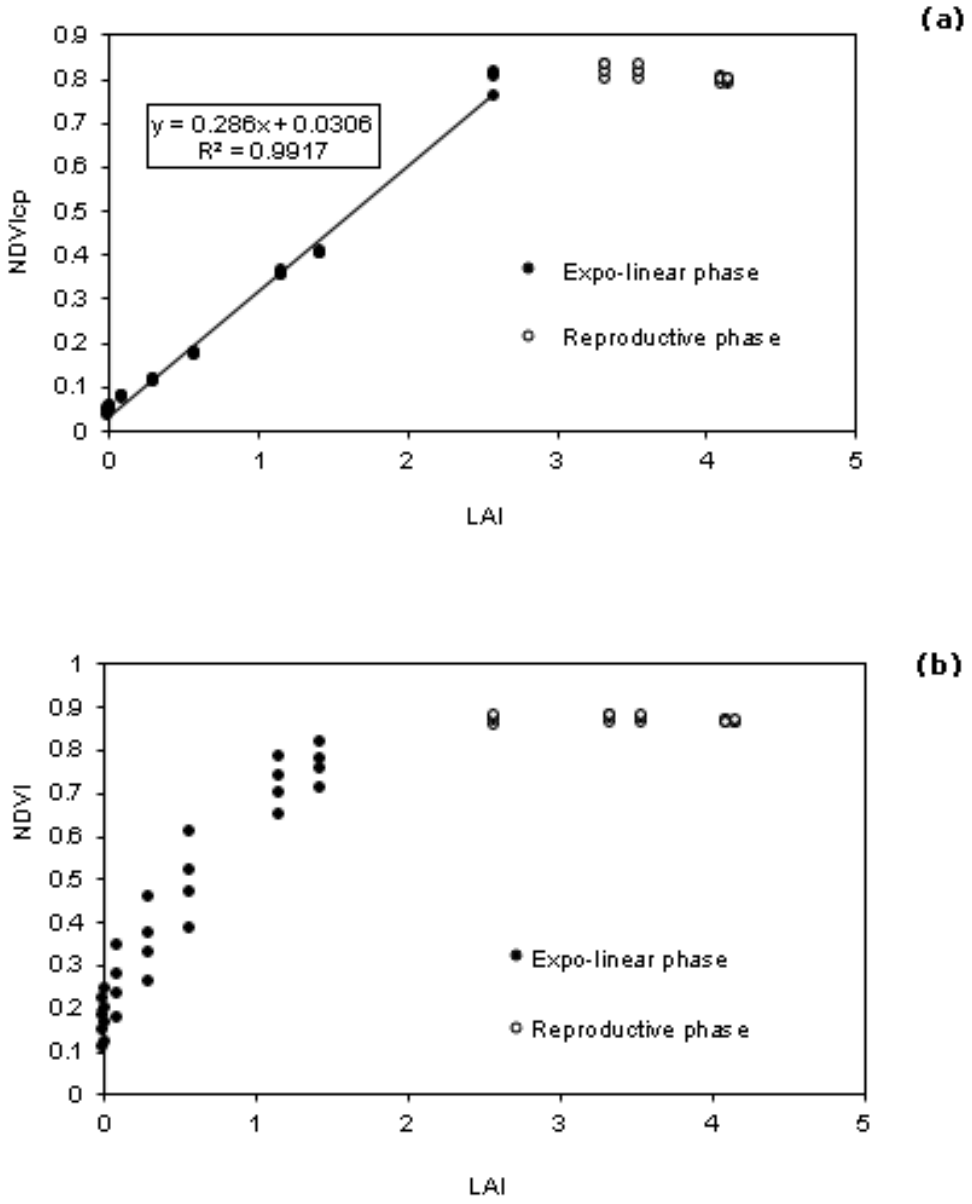

Figure 4. Results of applying spectral indices to the maize experiment. (a) $NDVI_{cp}$ and (b) $NDVI$.

Tecnología y ciencias del agua, ISSN 2007-2422, 13(3), 374-424. DOI: 10.24850/j-tyca-2022-03-08

Paz *et al*. (2014, 2015) have reviewed most VI published in the literature, concluding that none correctly approached the expo-linear pattern defined in Figure 2; this includes $NDVI_{cp}$, which was designed considering only the exponential pattern and its transition in the a_0-b_0 space. To achieve a complete approximation to the expo-linear pattern between a_0 and b_0 (Figure 2), Romero *et al*. (2009) used a transformation of the spectral spaces to develop the KIMO SAVI model to approximate the linear pattern to the shift to the exponential pattern (the opposite of $NDVI_{cp}$). Under this perspective, KIMO SAVI is defined in a format similar to that of $NDVI_{cp}$ (depending on b_0; Equation (2)), where KIMO SAVI = $NDVI_{cp}$ when b_0 is below a given threshold; KIMO SAVI is obtained from the transformed spectral space when b_0 is above the threshold (Romero *et al*., 2009; Paz *et al*., 2015).

Vegetation Spectral Indices and K_c

An estimate of the actual crop evapotranspiration as a function of the crop coefficient (mean K_c) (Doorenbos & Pruitt, 1977) and the reference evapotranspiration Et_0 has been proposed, as follows:

$$ETc = KcETo \quad (5)$$

Equation (5) refers to average conditions, so that Wright (1982) proposed the dual method for estimating K_c:

$$Kc = Kcb + Ke \quad (6)$$

Where K_{cb} is the baseline crop coefficient (no stress) and K_e is the coefficient associated with evaporation from the soil.

In crops subjected to water stress, the adjusted baseline crop coefficient, K_{cba}, is given by:

$$Kcba = (Kcb)(Ks) \quad (7)$$

The dual method and its adjustment for water stress are part of the current methodology proposed by FAO (Allen *et al*., 1998) using a virtual reference crop, and is the basis of the approximations for estimating ET_c using the crop coefficient.

To understand the limitations of the relationships between the various VI and K_c (K_{cb}, K_s, and K_e), Figure 5 shows radiative simulations

Tecnología y ciencias del agua, ISSN 2007-2422, 13(3), 374-424. DOI: 10.24850/j-tyca-2022-03-08

for maize under dry and wet soil, and an unstressed and stressed crop (Reyes *et al*., 2011).

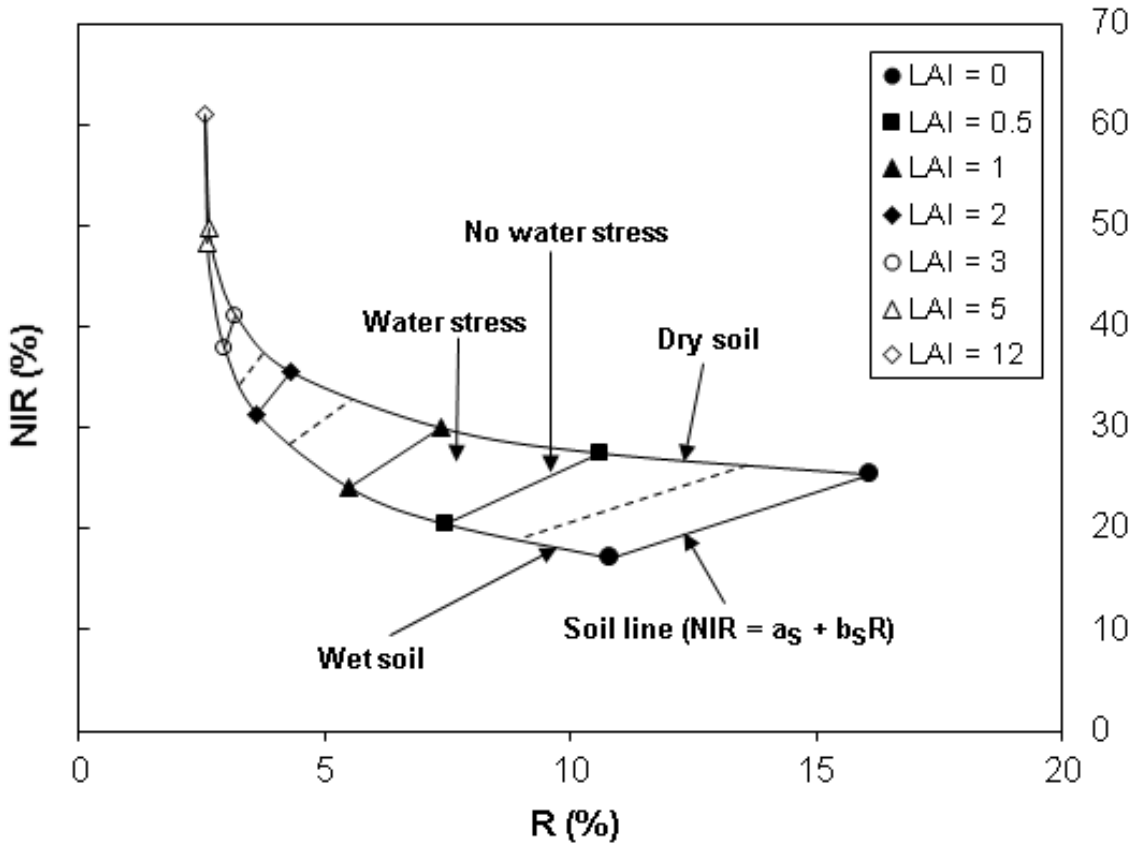

Figure 5. Radiative simulations of the maize crop under two soil moisture and water stress conditions.

Soil water content adjustment (K_e) is evident as different soil isolines (reduced *R* and *NIR* values), and water stress (K_s) as different *LAI*

Tecnología y ciencias del agua, ISSN 2007-2422, 13(3), 374-424. DOI: 10.24850/j-tyca-2022-03-08

isolines (lower slope of *LAI* isolines). Considering that the vast majority of VI intend to approximate the slope (or intersection) of *LAI* isolines (Paz *et al*., 2007; Paz *et al*., 2015), it is clear from Figure 5 that a "perfect" VI (direct and error-free estimate of the slope) cannot differentiate between K_{cb} and K_e (or K_c) because b_0 (or a_0) of *LAI* isolines contains no information on soil moisture content. Thus, the use of an VI that approximates b_0 or a_0 generates similar relationships for K_{cb}, $K_{cb} + K_e$, or K_c. This poses restrictions to the use of VI for estimating soil moisture, so soil isolines should be used for this purpose, at the level of transformed reflectance spaces (Paz *et al*., 2009) or with vegetation indices (Paz, Reyes, & Medrano, 2011).

Equivalent Radiative Media

On a crop plot, the *LAI* estimated experimentally represents a global one:

$$LAI_G = \left(\frac{\text{mean foliar area}}{\text{plant}}\right)\left(\frac{\text{number of plants}}{m^2 \text{ of the plot}}\right) \quad (8)$$

Without considering border effects, the local LAI_l (individual plants) is related to the global *LAI* as:

Tecnología y ciencias del agua, ISSN 2007-2422, 13(3), 374-424. DOI: 10.24850/j-tyca-2022-03-08

$$LAI_l = LAI_G fv \quad (9)$$

where *fv* is the fractional vegetation cover, ranging between 0 and 1. Thus, the fraction of soil cover is *fs* = 1 - *fv*.

Figure 6 shows LAI_l, where the fraction of gaps (*fh*) within the border of the foliage (horizontal projection) is given by the Beer-Lambert law for non-black leaves (Goudriaan & van Laar, 1994):

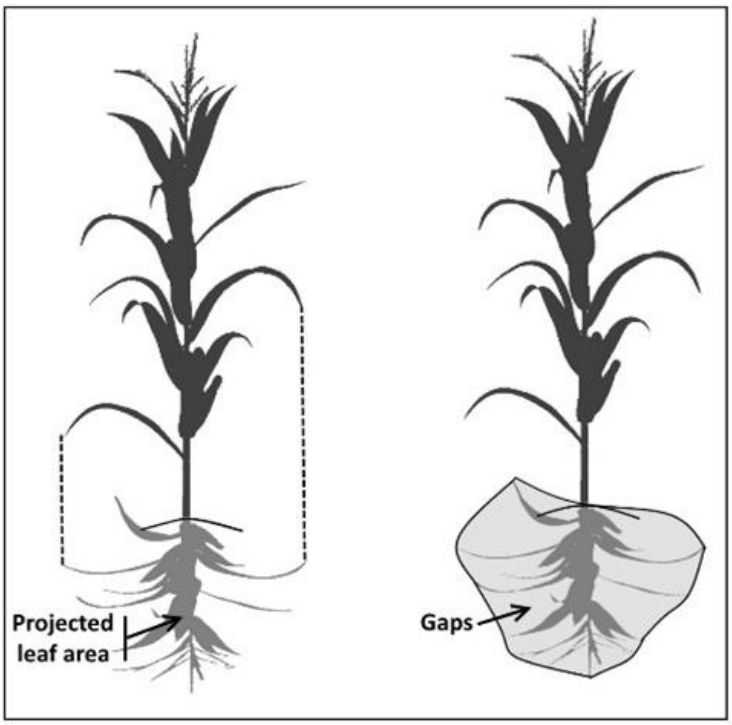

Figure 6. Leaf area and gaps for a local medium or an individual plant.

Tecnología y ciencias del agua, ISSN 2007-2422, 13(3), 374-424. DOI: 10.24850/j-tyca-2022-03-08

$$f_h = 1 - T_l \; ; \; T_l = exp\{(1-\omega)^{1/2} KxLAI_l\} \quad (10)$$

Where Tl is transmittance (local) of direct sun radiance, ω = ρ + τ is the leaf albedo (sum of leaf reflectance and transmittance, respectively), and K is the total extinction coefficient. Note that $fv \neq f_h$, since *fv* refers to the fraction of vegetation outside the boundaries of individual plants, although in practice (digital photographs) *fv* incorporates f_h.

Figure 7 shows a crop planted in furrows, where a pattern of individual plants appears in early growth stages, where plants do not overlap (case 3-D). As growth progresses, individual plants within a furrow overlap with each other and form a crop in rows or furrows (case 2-D). When plants from different rows overlap, a total soil coverage condition emerges (case 1-D). This growth dynamic requires a generic modeling approach that takes into account the geometric complexity of crops in plots as well as natural vegetation.

Tecnología y ciencias del agua, ISSN 2007-2422, 13(3), 374-424. DOI: 10.24850/j-tyca-2022-03-08

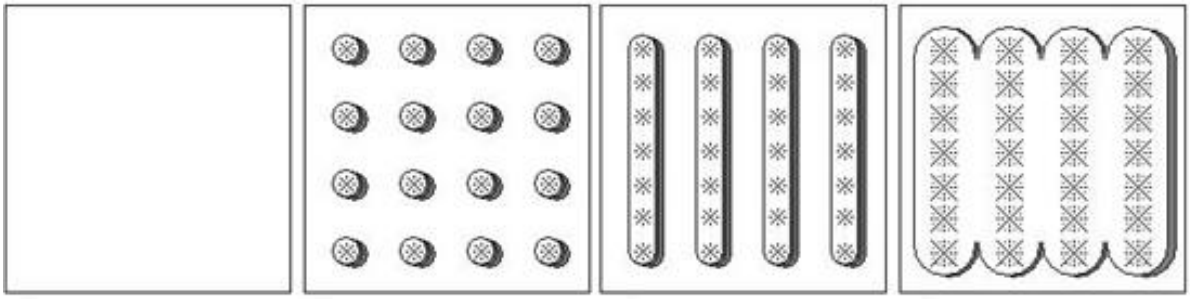

Figure 7. The geometry of a crop planted in furrows. (a) bare soil; (b) individual plants with no overlap; (c) plants overlapping within individual furrows; and (d) dense overlapping vegetation.

From the above analysis, an equivalent medium (physical terms) is one that meets the following (Paz *et al*., 2013):

$$LAI_G = \frac{LAI_l}{fv} \tag{11}$$

In other words, an LAI_G measurement involves an infinite number of equivalent combinations of LAI_l and fv that meet the Equation (11).

While an equivalent radiative medium has the same amount of plant elements, reflectances may differ depending on the amount of soil exposed and its moisture content. Thus, VI estimates and their relationship with fv and LAI_G are functions of the geometrical configuration

Tecnología y ciencias del agua, ISSN 2007-2422, 13(3), 374-424. DOI: 10.24850/j-tyca-2022-03-08

of soil and vegetation in a plot, as well as of the optical properties associated with it.

The discussion of equivalent radiative media (Equation (11)) is essential to understand the limitations in the use of *fv* or LAI_G to indirectly estimate K_c (or K_{cb}), as proposed in FAO-56 (Allen *et al*., 1998). This method uses an *fv* = 10 % to define the beginning of the vegetative growth stage, whose end is given by an *fv* of 70-80 % or a *LAI* of 2-3 (Allen *et al*., 1998). From Equation (11), it is clear that an LAI_I (*fv* and LAI_G) should be defined to uniquely associate the geometry and amount of vegetation (stomates) in a plot, since the definition of a single value, *fv* or LAI_G, is insufficient to characterize the medium (Odi-Lara, Paz-Pellat, López-Urrea, & González-Piqueras, 2013). This issue is evident in the definition of "effective coverage" (end of the vegetative phase), where fixed *fv* or LAI_G values are associated with it (Allen *et al*., 1998). This implies a standardized crop in terms of sowing geometry that ignores the basic architecture of plants and their geometric distribution within plots. Consequently, the effective coverage can be expressed as *fv* or LAI_G values that may differ substantially from those recommended by FAO-56 (Allen *et al*., 1998).

Materials and methods

Tecnología y ciencias del agua, ISSN 2007-2422, 13(3), 374-424. DOI: 10.24850/j-tyca-2022-03-08

Two crops with average leaf density were analyzed: maize (*Zea mays* L.) var. Dracma 700 (Calera, González-Piqueras, & Meliá, 2004; González-Piqueras, Calera, Gilabert, Cuesta, & De-la- Cruz, 2004) and wheat (*Triticum aestivum* L.) var. Estero (López-Urrea, Montoro, González-Piqueras, López-Fuster, & Fereres, 2009a). The variables measured were *LAI*, *fv*, *Bm* (aerial dry biomass), and *h*, in addition to spectral measures and evapotranspiration in a weighing lysimeter.

The experiments were carried out at *Instituto Técnico Agronómico Provincial*, Albacete, Spain (39º14' N, 2º5'E, 695 m.a.s.l.) in years 2001 and 2003 for maize and wheat, respectively. The climate is continental semi-arid, with a mean annual precipitation of 320 mm, mostly in spring and autumn. Mean, maximum, and minimum temperatures are 13.7, 24.0, and 4.5 °C; respectively (López-Urrea *et al*., 2006a; López-Urrea *et al*., 2009a). The soil was classified as Petrocalcic Calcixerepts (Soil Survey Staff, 2006). The mean depth is 40 cm, delimited by a moderately fragmented petrocalcic horizon. The texture is silty clay loam, with 13.42 % sand, 48.89 % silt, and 31.60 % clay; the pH is alkaline. The soil has low organic matter and total nitrogen content, and high levels of active lime and potassium. The volumetric water content was 0.34 m^3 m^{-3} at field capacity (FC) and 0.21 m^3 m^{-3} at the permanent wilting point (PWP). For wheat, the estimated usable moisture for a root zone of 35 cm was

Tecnología y ciencias del agua, ISSN 2007-2422, 13(3), 374-424. DOI: 10.24850/j-tyca-2022-03-08

45.5 mm; a maximum permissible depletion level of 0.55 was used for the irrigation schedule, as recommended by Allen *et al*. (1998) for wheat for an ET_c of 5 mm d^{-1}.

Crops were grown under optimal conditions, with no restriction of water or nutrients. Wheat was fertilized after planting, by adding 28 kg ha^{-1} N, 112 kg ha^{-1} P_2O_5, and 70 kg ha^{-1} K_2O; liquid fertilizer was applied in the vegetative phase (170 kg ha^{-1} N). The plot was irrigated by spraying through total buried coverage. All efforts were made for the lysimeter crop to maintain the same growth rate and plant density as the protection plot.

Crop evapotranspiration was measured with a weighing lysimeter with continuous data recording placed at the center of a 100 x 100 m plot (López-Urrea *et al.*, 2006a). The lysimeter measured 2.7 m long, 2.3 m wide, and 1.7 m deep, with a total mass of 14.5 t The load cell has a 0.25 kg resolution, equivalent to 0.04 mm of water. Evapotranspiration was estimated from the weight data recorded by the lysimeter, as

$$ET = P + R - D \pm \Delta w \qquad (12)$$

where P is precipitation, R is irrigation, D is drainage, and Δw corresponds to variations in water content in the soil mass.

The daily amount of evaporated water was calculated based on hourly data. When the daily value could not be obtained for any reason

Tecnología y ciencias del agua, ISSN 2007-2422, 13(3), 374-424. DOI: 10.24850/j-tyca-2022-03-08

(rain, irrigation, maintenance), the value used was the average of those for the previous and following days. Other sources of error that led to data elimination were weight check, calibrations for loss of contact in the load cell, low system voltage, loss of contact of the ground cable, and failure of the data controller (López-Urrea *et al.*, 2006a).

ET_o was calculated using the FAO-56 Penman-Monteith equation (Allen *et al*., 1998), which has yielded better results for the area of interest in previous studies (López-Urrea *et al*., 2006a; López-Urrea *et al*., 2006b). Climate data were obtained from a weather station located on the experimental farm. Missing net radiation, wind speed, and relative humidity data were estimated using the previous data. The integration time considered was one hour, and daily figures were calculated from these data.

Spectral measurements were done using a GER 3700 radiometer (Spectra Vista Corporation, NY, USA) with a spectral range of 300-2500 nm and a maximum spectral resolution of 1.5 nm. The observation height to record plant cover was 1.80 m for wheat and 5 m for maize, allowing an observation diameter of 21 and 58 cm, respectively, for a 6.6º field of view (FOV).

Each crop was monitored at regular intervals (7-10 days). For maize, a 6-point transect was measured inside and outside of the lysimeter to ensure that it was representative of the plot; for wheat, 5 measures along the lysimeter were recorded. Measures were taken during maximum solar elevation and on clear days (no clouds), and nadir

observations were made (Milton, 1987). Reflectance was calibrated using a Spectralon (Labsphere™) reference panel before each surface measurement to avoid variations in the illumination setting (McCoy, 2005).

The phenology of each crop was recorded. Table 1 details the development stages.

Table 1. Maize and wheat phenology.

Maize, 2001		**Wheat, 2003**	
Julian Day	Phenology	Julian Day	Phenology
104	Sowing	41	Sowing
116	Emergence	56	Emergence
164	V5	71	Two leaves
171	V6	77	Three leaves
178	V7	84	Onset of tillering
185	V9	92	Tillering
193	V11	114	Straightening - one node
201	V14	120	Two nodes

Tecnología y ciencias del agua, ISSN 2007-2422, 13(3), 374-424. DOI: 10.24850/j-tyca-2022-03-08

207	Male flower	134	Emergence of ear
213	Fertilization	141	Free ear
219	Fertilization	148	Milky ripening
225	Milky	153	Pasty ripening
241	Milky-pasty	163	Over-ripening
249	Pasty	171	Hard grain
256	Vitreous		
263	Vitreous		
272	Vitreous		
277	Physiological ripening		

The fractional vegetation cover *fv* was estimated using the supervised classification technique (maximum likelihood) from digital photographs taken at the nadir of the cover. Images were classified with the program ENVI^{TM}, differentiating between green vegetation and soil.

To calculate the leaf area index, *LAI*, a 1 m^2 sample was collected from the protection plot; then, one side of each leave was measured with a LI COR^{MR} *LAI* 3000 instrument.

Following the FAO guidelines, crop height was measured to adjust the crop coefficient (K_c) values throughout the growth cycle. Crop height

Tecnología y ciencias del agua, ISSN 2007-2422, 13(3), 374-424. DOI: 10.24850/j-tyca-2022-03-08

was measured from the base to the highest element of the plant, with plants selected at random in the protection plot.

Results and discussion

Estimating K_c (K_{cb} + K_e) or K_{cb} (indistinguishable in terms of VI) at the agricultural farm or plot level requires that the effect of soil (water content) be brought to a minimum. When considering a precision irrigation scheme, it is important to determine the spatial variability of K_c (ET_c) to attain an efficient use of water resources.

Figure 8 shows the estimated *NDVI* for different Julian days, evidencing that this index is ineffective for reducing the effects of soil. Thus, the use of an average *NDVI* is an arbitrary decision, since, for a given day, soil moisture at the time of measurements remains relatively constant; hence, any variations are attributable solely to the inability of *NDVI* to minimize the effect of soil and/or the variations in the crop condition. On the other hand, *NDVI* shows saturation issues (remains constant over time) before the crop reaches the peak *LAI* or *fv*, thus restraining its use only to the exponential vegetative growth phase,

Tecnología y ciencias del agua, ISSN 2007-2422, 13(3), 374-424. DOI: 10.24850/j-tyca-2022-03-08

without considering the linear phase. The use of *NDVI* to estimate K_c (Castañeda-Ibáñez *et al*., 2015; Palacios-Vélez, Palacios-Sánchez, & Espinosa-Espinosa, 2018) is not supported, since having statistically acceptable empirical relationships between an VI and K_c is not sufficient; its use requires the right answers for the right reasons (Kirchner, 2006). A poor understanding of the radiative transfer concepts associated with VI strongly limits empirical approaches, which are supported only by arbitrary statistical adjustments. Due to the use of the photosynthetic (R) and non-photosynthetic (NIR) bands, any VI is expected to approach, albeit roughly, the growth of a crop and, thus, the evolution of K_c.

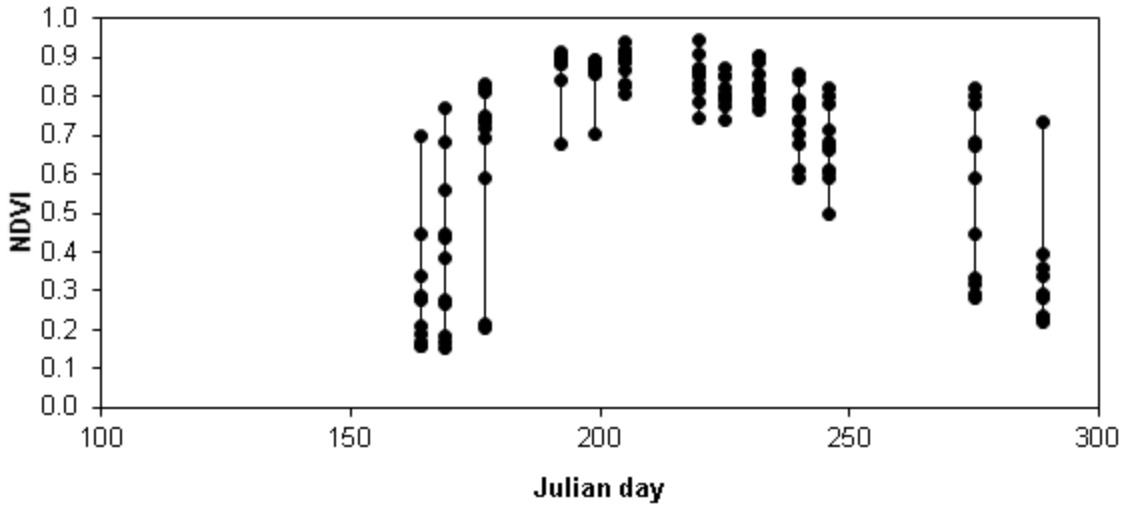

Figure 8. Variation of *NDVI* through time for maize lysimeter measurements.

Tecnología y ciencias del agua, ISSN 2007-2422, 13(3), 374-424. DOI: 10.24850/j-tyca-2022-03-08

The highest variations at the beginning and end of the maize growth cycle, as shown in Figure 8, reflect the condition of vegetation with low soil cover, so that the effect of soil predominates.

To avoid the issue of approximating the slopes of *LAI* isolines in the R-NIR space, these were estimated directly from spectral data (no soil effect). From the b_0 slopes estimated for different days of the growth cycle of maize and wheat, the KIMO SAVI was estimated, which represents the whole cycle. Also, lysimeter K_c measurements were reviewed to select K_{cb} values (the lowest values) from the temporal K_c pattern. Figure 9 shows the temporal patterns of K_{cb} and KIMO SAVI for maize and wheat crops, showing a lag between biophysical growth, represented by KIMO SAVI, and the one associated with the current evapotranspiration, as there is a linear relationship between the former and *LAI* (Paz *et al*., 2007; Romero *et al*., 2009).

Tecnología y ciencias del agua, ISSN 2007-2422, 13(3), 374-424. DOI: 10.24850/j-tyca-2022-03-08

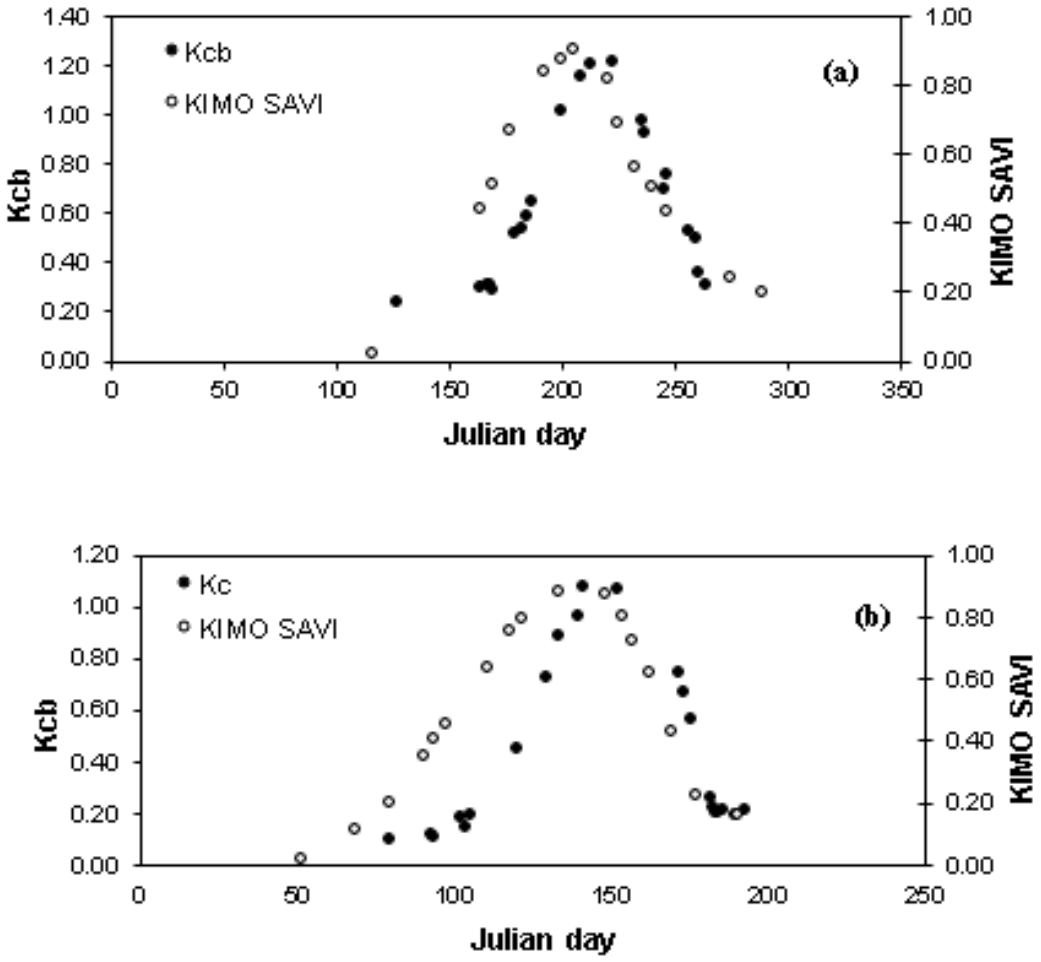

Figure 9. K_{cb} and KIMO SAVI temporal patterns: (a) maize; (b) wheat.

Figure 10 illustrates the linear relationships between KIMO SAVI and K_{cb}, clearly showing one relationship for the vegetative phase and another for senescence, with constant K_{cb} values (plateau) between the two phases (solid squares in Figure 10). The parameters of the linear

Tecnología y ciencias del agua, ISSN 2007-2422, 13(3), 374-424. DOI: 10.24850/j-tyca-2022-03-08

relationships differ between the vegetative and senescence phases; therefore, a single linear relationship cannot be used, as opposed to proposals by different authors (Bausch, 1993; González-Piqueras *et al*., 2004; López-Urrea, De-Santa-Olalla, Fabeiro, & Moratalla, 2009b; Palacios-Vélez *et al*., 2018).

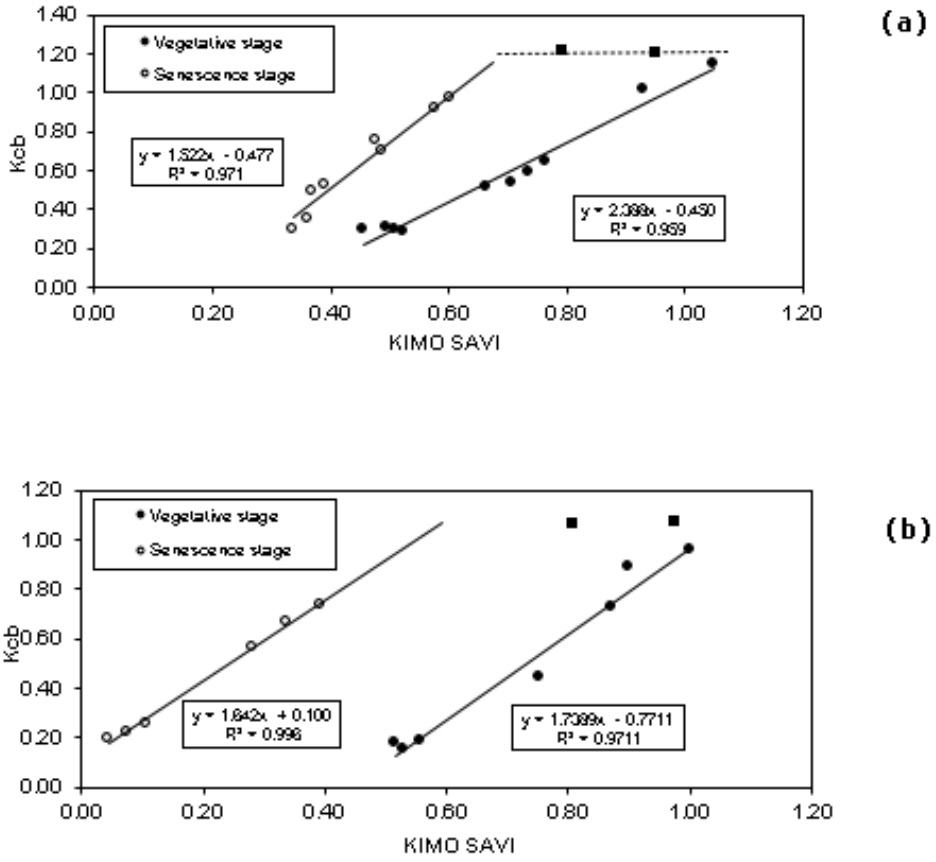

Figure 10. Relationships between KIMO SAVI and K_{cb}: (a) maize; (b) wheat.

Tecnología y ciencias del agua, ISSN 2007-2422, 13(3), 374-424. DOI: 10.24850/j-tyca-2022-03-08

Figure 11 depicts linear relationships between IV_KIMO SAVI and *LAI* for maize crops, showing relationships like those for K_{cb}. Thus, the parameterization of K_c or K_{cb} as a function of *fv* or *LAI* is equivalent to that of KIMO SAVI. Given the issues in using only *LAI* (or *fv*), the relationships with K_c or K_{cb} vary according to the local conditions, i.e., the parameters of the linear relationships depend on the crop-planting geometry and development plant stage.

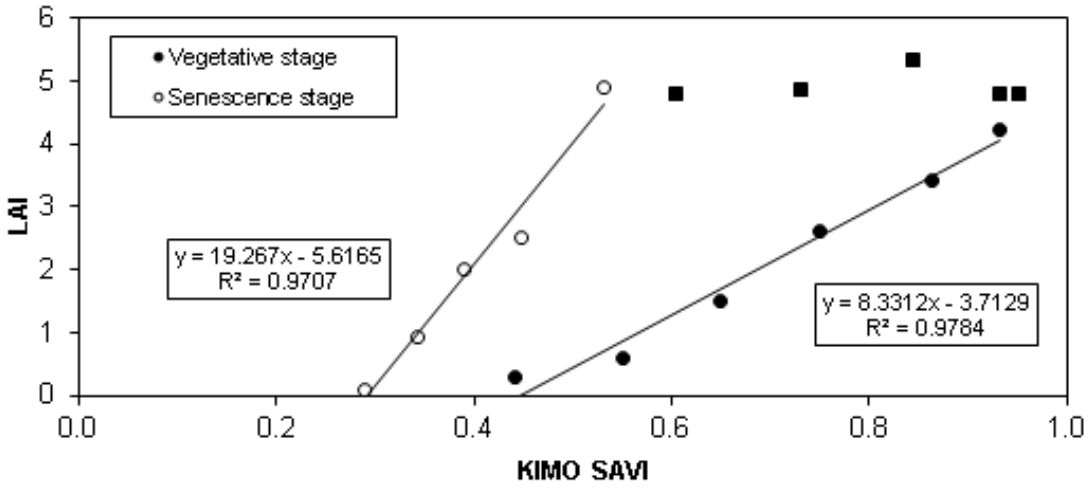

Figure 11. Relationships of KIMO SAVI with *LAI*.

The analysis of the issues associated with the use of *fv* and *LAI* separately reveals the need to define the beginning and end (effective

Tecnología y ciencias del agua, ISSN 2007-2422, 13(3), 374-424. DOI: 10.24850/j-tyca-2022-03-08

coverage) of the vegetative phase to parameterize the relationship with KIMO SAVI. In this regard, a direct estimate of the beginning and end using KIMO SAVI temporal patterns is required; the expo-linear model in Equation (1) can be used for this purpose, given the linear relationship between KIMO SAVI and *LAI* (Odi-Lara *et al*., 2013). Thus, by defining the beginning and end of the vegetative phase as t_T and t_{MAX}, respectively, KIMO SAVI for those time points can be used to define the K_{cb} or K_c values associated with those stages (FAO-56 data or lysimeter estimates), so that the pair of points are used to determine the parameters of the linear relationship. Now, considering that based on KIMO SAVI the vegetative phase is represented by the linear phase (with the start of the shift from exponential to linear) and that the temporal relationship of K_c or K_{cb} tends to be nonlinear (exponential), Figure 9, a logarithmic-exponential transformation can be used to make both patterns equivalent (*i* means initial; *f* means final):

$$f = \frac{ln(Kcb,i) - ln(Kcb,f)}{KIMO\ SAVI_i - KIMO\ SAVI_f};\ e = ln(Kcb,f) - fxIV\_CIMASf\ ;\ Kcb = exp(e + fxKIMO\ SAVI) \quad (13)$$

Using Equation (13), Figure 12 shows the relationship between estimated and lysimeter K_{cb} values for maize and wheat, using the lysimeter values to parameterize Equation (13).

Tecnología y ciencias del agua, ISSN 2007-2422, 13(3), 374-424. DOI: 10.24850/j-tyca-2022-03-08

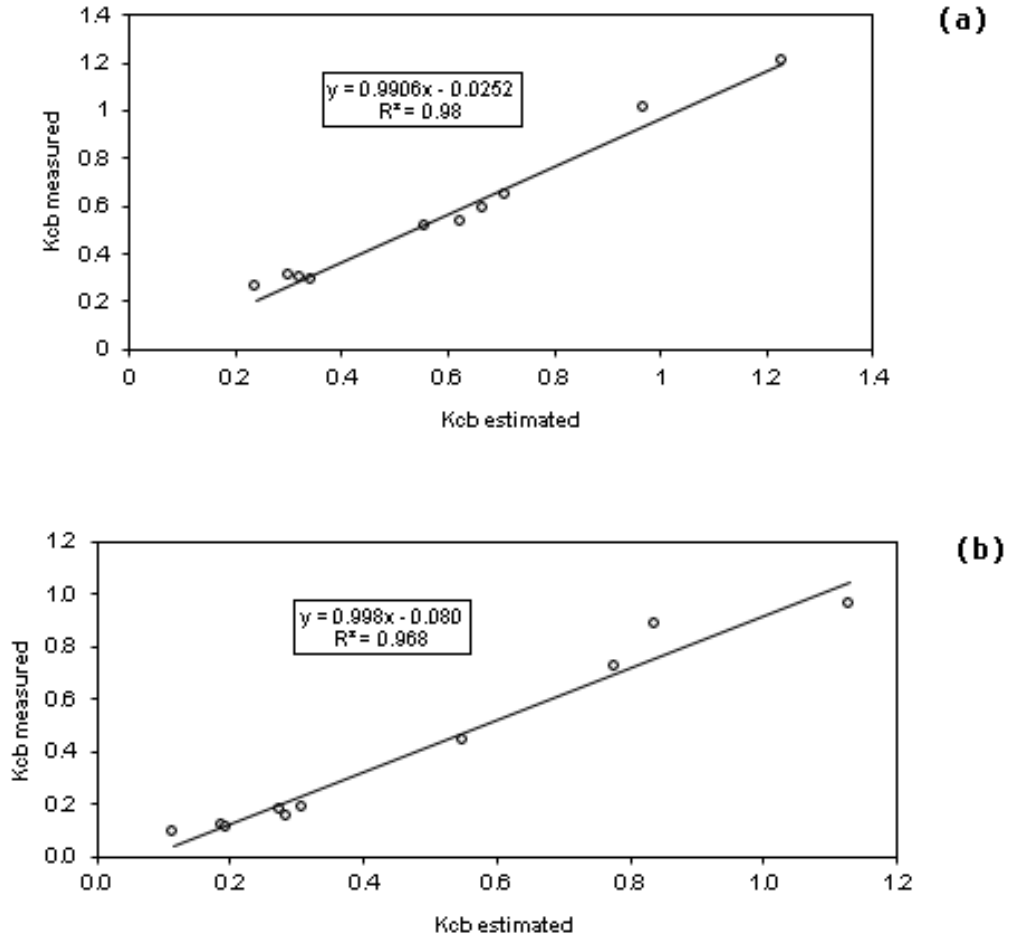

Figure 12. Relationship between estimated and measured K_{cb}: (a) maize; (b) wheat.

Tecnología y ciencias del agua, ISSN 2007-2422, 13(3), 374-424. DOI: 10.24850/j-tyca-2022-03-08

The relationship between the estimated K_{cb} (Equation (13)) and the values measured depicted in Figure 12 shows that the estimate with two data pairs for auto-calibrating KIMO SAVI yields good results and can be used in operational terms. The relationship between KIMO SAVI and K_{cb} is similar for K_c; therefore, we can use K_c values at the beginning and end of the vegetative (linear) phase in Equation (13) to obtain K_c estimates for this phase. The initial value (time before t_T) is constant and equal to $K_{cb,i}$ or $K_{c,i}$.

Something like the vegetative phase can be applied to the senescence phase, thereby defining a methodology that can be auto-calibrated (FAO-56 tables or field measurements) to define the relationship between KIMO SAVI and K_{cb} or K_c.

The advantage of the proposed methodology is that it is independent of atmospheric effects, as it is calibrated with local KIMO SAVI estimates and the K_{cb} or K_c values used as the beginning and end of a phase. Assuming relatively similar effects within a growth cycle, or considering their minimization, these estimates are suitable for use in applications at quasi-real-time under the hypotheses or restrictions associated with the FAO-56 methodology.

Relationship between KIMO SAVI and Aerial Biomass

Figure 13 shows the relationship between dry aerial biomass (*Bm*) and KIMO SAVI for maize and wheat, where an exponential relationship between KIMO SAVI and Bm is obtained for the vegetative phase (and the plateau). Something similar is observed for the senescence phase. In other words, using KIMO SAVI *versus* ln (*Bm*) leads to two linear relationships that intersect at the start of the senescence phase.

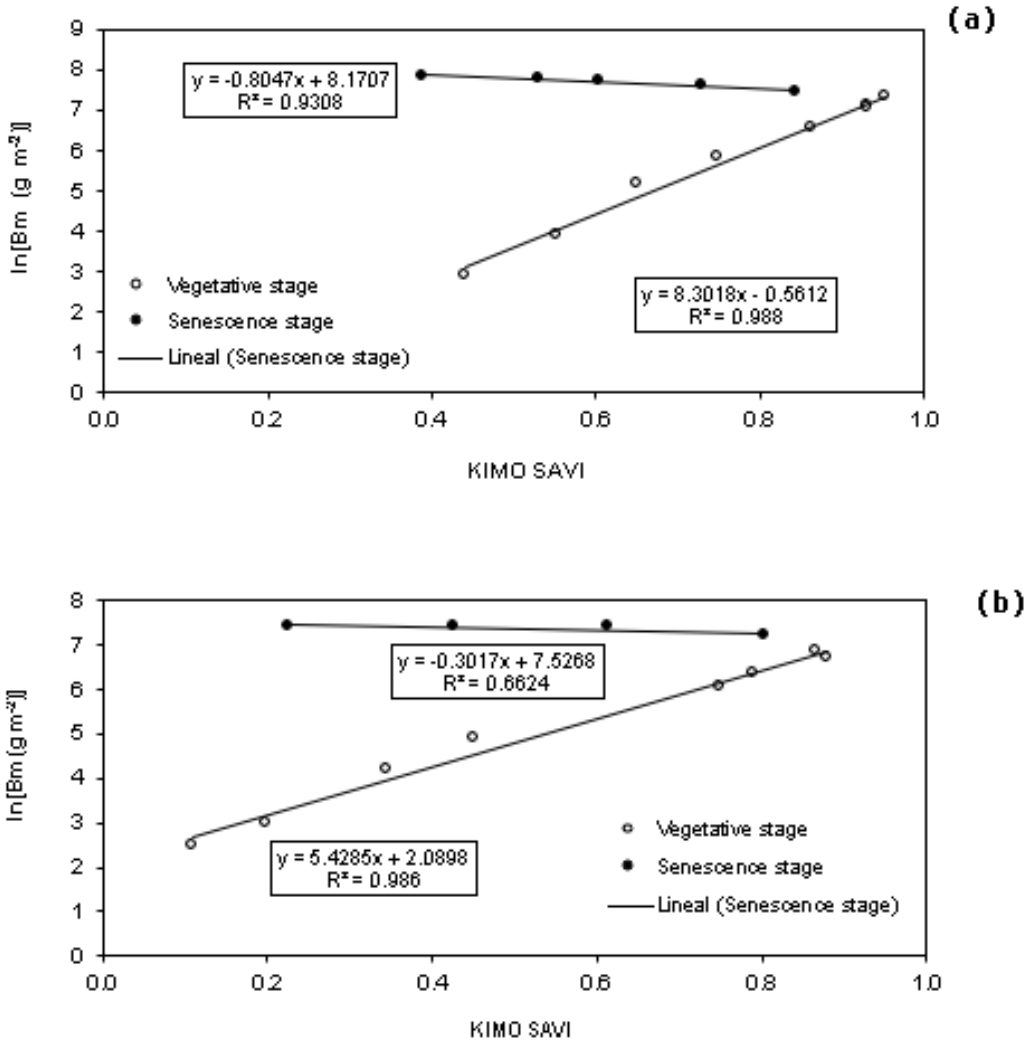

Figure 13. Relationships between KIMO SAVI and dry *Bm*: (a) maize; (b) wheat.

Tecnología y ciencias del agua, ISSN 2007-2422, 13(3), 374-424. DOI: 10.24850/j-tyca-2022-03-08

Conclusions

This paper outlines the scope and limitations of the use of spectral vegetation indices (VI) for estimating the crop coefficients (K_c or K_{cb}) of the FAO-56 methodology.

Considering that VI aims to approximate the slope b_0, or the intercept a_0, of *LAI* isolines of crops, it was clarified that the relationships between an VI and K_{cb} or K_c are equivalent since by definition *LAI* isolines cannot estimate soil moisture. The latter requires the use of soil isolines, as discussed by Paz *et al*. (2009).

Under the assumption of equivalent radiative media (spectral spaces), the separate use of the fractional coverage (*fv*) or the global leaf area index (*LAI*) generates multiple solutions to the definition of starting and end of K_c phases according to FAO-56. The parameterization of these time points requires the joint consideration of *LAI* and *fv* to reflect the geometry of crop planting.

Using the generic format of the KIMO SAVI index along with direct estimates of the slopes of *LAI* isolines in two experiments (maize and wheat), linear relationships were obtained between K_{cb} and KIMO SAVI

Tecnología y ciencias del agua, ISSN 2007-2422, 13(3), 374-424. DOI: 10.24850/j-tyca-2022-03-08

for the vegetative and senescence phases. This implies that using a single relationship between VI and K_c or K_{cb} is incorrect. Given this constraint that requires local calibrations with field measurements, this work proposes a methodology for the direct estimation of the relationship between KIMO SAVI and either K_{cb} or K_c for use in operational terms.

The analyses reported herein underline the limitations in estimating K_c or K_{cb} given the intrinsic limitation of the conventional VI design to approximate the slopes of *LAI* isolines. Thus, under this consideration, VI cannot be used to approximate K_e (soil moisture). Notwithstanding the above, K_{cb} affected by water stress (assessed by any means), *i.e.*, $K_{cb}*K_s$, can be estimated similarly to unstressed K_{cb}, provided the initial and final $K_{cb}*K_s$ values associated with the stages of the FAO-56 methodology are available. This aspect deserves further investigation.

Acknowledgments

The authors thank Dr. José Gonzalez-Piqueras and Dr. Ramon López-Urrea for the kind authorization for the use of data from their field campaigns in Spain.

References

Allen, R. G., Pereira, L. S., Raes, D., & Smith, M. (1998). *Crop evapotranspiration. Guidelines for computing crop water*

requirements. FAO Irrigation and Drainage Paper No. 56. Rome, Italy: FAO. Recovered from http://www.fao.org/3/x0490e/x0490e00.htm

Allen, R. G., Tasumi, M., & Trezza, R. (2005). *METRIC: mapping evapotranspiration at high resolution – Applications manual for LANDSAT satellite image*. Idaho, USA: University of Idaho.

Bastiaanssen, W. G. M., Menenti, M., Feddes, R. A., & Holtslag, A. A. M. (1998). A remote sensing surface energy balance algorithm for land (SEBAL): 1. Formulation. *Journal of Hydrology*, 212–213(1-4), 198-212. Recovered from https://doi.org/10.1016/S0022-1694(98)00253-4

Bausch, W. C. (1995). Remote sensing of crop coefficients for improving the irrigation scheduling of corn. *Agricultural Water Management*, 27, 55-68. Recovered from https://doi.org/10.1016/0378-3774(95)01125-3

Bausch, W. C. (1993). Soil background effects on reflectance-based crop coefficients for corn. *Remote Sensing of Environment*, 46, 213-222. Recovered from https://doi.org/10.1016/0034-4257(93)90096-G

Bausch, W. C., & Neale, C. M. U. (1989). Spectral inputs improve corn crop coefficients and irrigation scheduling. *Transactions of the ASAE*, 46, 1901-1908.

Bausch, W. C., & Neale, C. M. U. (1987). Crop coefficients derived from reflected canopy radiation: A concept. *Transactions of the ASAE*, 30, 703-709.

Calera, A., González-Piqueras, J., & Meliá, J. (2004). Monitoring barley and corn growth from remote sensing data at field scale. *International Journal of Remote Sensing*, 25, 97-109. DOI: 10.1080/0143116031000115319

Calera, A., Jochum, A. M., Cuesta, A., Montoro, A., & Fuster, P. L. (2005). Irrigation management from space: towards user-friendly products. *Irrigation Drainage Systems*, 19, 337-353.

Castañeda-Ibáñez, C. R., Martínez-Menes, M., Pascual-Ramírez, F., Flores-Magdaleno, H., Férnandez-Reynoso, D. & Esparza-Govea, S. (2015). Estimation of crop coefficients through remote sensing in the Río Yaqui irrigation district, Sonora, México. *Agrociencia*, 49, 2, 221-232. Recovered from https://agrociencia-colpos.mx/index.php/agrociencia/issue/view/108.

Choudhury, B. J., & Monteith, J. L. (1988). A four-layer model for the heat budget of homogeneous land surfaces. *Quarterly Journal of the Royal Meteorological Society*, 114, 373-398. Recovered from https://doi.org/10.1002/qj.49711448006.

Doorenbos, J., & Pruitt, W. O. (1977). *Guidelines for predicting crop water requirements. FAO Irrigation and Drainage Paper*. Vol. 24. Rome, Italy: The Food and Agriculture Organization.

Ferrandino, F. J. (1989). Spatial and temporal variation of a defoliating plant disease and reduction in yield. *Agricultural and Forest Meteorology*, 47, 273-289.

Gilabert, M. A., González-Piqueras, J., García-Haro, F. J., & Meliá, J. (2002). A generalized soil-adjusted vegetation index. *Remote Sensing of Environment*, 82, 303-310. Recovered from https://doi.org/10.1016/S0034-4257(02)00048-2

González-Piqueras, J., Calera, A., Gilabert, M. A., Cuesta, A., & De-la-Cruz, F. (2004). Estimation of crop coefficients by means of optimized vegetation indices for corn. *Proceedings SPIE*, 5232, 110-118. Recovered from https://doi.org/10.1117/12.511317

Goudriaan, J., & Monteith, J. L. (1990). A mathematical function for crop growth based on light interception and leaf area expansion. *Annals of Botany*, 66, 695-701. Recovered from https://doi.org/10.1093/oxfordjournals.aob.a088084.

Goudriaan, J., & van Laar, H. H. (1994). *Modelling potential crop growth processes. Textbook with exercises*. Current Issues in Production Ecology. Dordrecht, The Netherlands: Kluwer Academic Publishers.

Heilman, J. L., Heilman, W. E., & Moore, D. G. (1982). Evaluating the crop coefficient using spectral reflectance. *Agronomy Journal*, 74, 967-971. Recovered from https://doi.org/10.2134/agronj1982.00021962007400060010x.

Jackson, R. D., Pinter, P. J., Reginato, R. J., & Idso, S. B. (1980*). Hand-held radiometry. A set of notes developed for use at the workshop on hand-held radiometry*. Phoenix, USA: US Department of Agriculture, Agricultural Reviews and Manuals.

Kirchner, J. W. (2006). Getting the right answers for the right reasons: Linking measurements, analyses, and models to advance the science of hydrology. *Water Resources Research*. DOI: 10.1029/2005WR004362

López-Urrea, R., Montoro, A., González-Piqueras, J., López-Fuster, P., & Fereres, E. (2009a). Water use of spring wheat to raise water productivity. *Agricultural Water Management*, 96, 1305-1310. DOI: 10.1016/j.agwat.2009.04.015

López-Urrea, R., Montoro, A., López-Fuster, P., & Fereres, E. (2009b). Evapotranspiration and responses to irrigation of broccoli. *Agricultural Water Management*, 96, 1155-1161. DOI: 10.1016/j.agwat.2009.03.011

López-Urrea, R., De-Santa-Olalla, F. M., Fabeiro, F., & Moratalla, A. (2006a). Testing evapotranspiration equations using lysimeter observations in a semiarid climate. *Agricultural Water Management,* 85, 15-26.

López-Urrea, R., De-Santa-Olalla, F. M., Fabeiro, C., & Moratalla, A. (2006b). An evaluation of two hourly reference evapotranspiration equations for semiarid conditions. *Agricultural Water Management,* 86, 277-282. Recovered from https://doi.org/10.1016/j.agwat.2006.05.017

McCoy, R. M. (2005). *Fields methods in remote sensing*. New York, USA: The Guilford Press. Recovered from https://doi.org/10.1111/j.1541-0064.2006.00161_2.x

Milton, E. J. (1987). Principles of field spectroscopy. *International Journal of Remote Sensing*, 8, 1807-1827.

Odi, M., Paz, F., & Bolaños, M. (2010). Limitations in the estimation of biophysical variables in crops using spectral vegetation indexes: Foliage density effect. *Agrociencia*, 44, 807-819.

Odi-Lara, M., Paz-Pellat, F., López-Urrea, R., & González-Piqueras, J. (2013). Definición de la etapa de desarrollo de los cultivos para estimar evapotranspiración usando la metodología FAO-56 y sensores remotos. *Tecnología y ciencias del agua*, 4, 87-102.

Palacios-Vélez, E., Palacios-Sánchez, L. A., & Espinosa-Espinosa, J. L. (2018). Evaluation of water use efficiency in irrigated agriculture supported by satellite images. *Tecnología y ciencias del agua*, 9, 31-38. DOI: https://doi.org/10.24850/j-tyca-2018-01-02

Paz, F., Romero, E., Palacios, E., Bolaños, M., Valdez, R., & Aldrete, A. (2015). Alcances y limitaciones de los índices espectrales de la vegetación: análisis de índices de banda ancha. *Terra Latinoamericana*, 33(1), 27-49. Recovered from https://www.terralatinoamericana.org.mx/index.php/terra/article/view/43

Paz, F., Romero, E., Palacios, E., Bolaños, M., Valdez, R., & Aldrete, A. (2014). Alcances y limitaciones de los índices espectrales de la vegetación: marco teórico. *Terra Latinoamericana*, 32(3), 177-194. Recovered from https://www.terralatinoamericana.org.mx/index.php/terra/article/view/22

Paz, F., Casiano, M., Zarco, A., & Bolaños, M. (2013). Estimación de las propiedades ópticas de la vegetación usando medios radiativos equivalentes y espacios n-paramétricos. *Terra Latinoamericana*, 31, 119-134.

Paz, F., Reyes, M., & Medrano, E. (2011). Design of spectral vegetation indexes using iso–soil curves. *Agrociencia*, 45, 121-134.

Paz, F., Marin, M. A., López, E., Zarco, A., Bolaños, M. A., Oropeza, J. L., Martínez, M., Palacios, E., & Rubiños, E. (2009). Elementos para el desarrollo de una hidrología operacional con sensores remotos: mezcla suelo-vegetación. *Ingeniería Hidráulica en México*, 14, 69-80.

Paz, F., Palacios, E., Bolaños, M., Palacios, L. A., Martínez, M., Mejía, E., & Huete, A. (2007). Design of a vegetation spectral index: NDVIcp. *Agrociencia*, 41, 539-554.

Paz, F., Palacios, E., Mejía, E., Martínez, M., & Palacios, L. A. (2005). Analysis of the spectral spaces of reflectance from crop canopies.

Agrociencia, 39, 293-301. Recovered from https://www.redalyc.org/pdf/302/30239306.pdf

Reyes, M., Paz, F., Casiano, M., Pascual, F., Marín, M. I., & Rubiños, E. (2011). Characterization of stress effect using spectral vegetation indexes for the estimate of variables related to aerial biomass. *Agrociencia, 45*, 221-233. Recovered from http://www.scielo.org.mx/pdf/agro/v45n2/v45n2a7.pdf.

Romero, E., Paz, F., Palacios, E., Bolaños, M., Valdez, R., & Aldrete, A. (2009). Design of a spectral vegetation index under the joint perspective of exponential and linear growth patterns. *Agrociencia*, 43, 291-307.

Ross, J. (1981). *The radiation regime and architecture of plant stands*. Norwell, USA: W. Junk. DOI: 10.1007/978-94-009-8647-3

Rouse, J. W., Haas, R. H., Schell, J. A., Deering, D. W., & Harlan, J. C. (1974). *Monitoring the vernal advancement of retrogradation of natural vegetation*. Type III, Final Report. Greenbelt, USA: NASA/GSFC.

Shuttleworth, W. J., & Wallace, J. S. (1985). Evaporation from sparse crops – An energy combination theory. *Quarterly Journal of the Royal Meteorological Society*, 111, 839-855. Recovered from http://facetas.sdsu.edu/shuttleworthwallace.pdf

Soil Survey Staff. (2006). *Keys to Soil Taxonomy* (10th ed.). Washington, DC, USA: USDA-Natural Resources Conservation Service.

Recovered from https://www.nrcs.usda.gov/Internet/FSE_DOCUMENTS/nrcs142p2_052172.pdf

Tucker, C. J. (1979). Red and photographics infrared linear combination for monitoring vegetation. *Remote Sensing of Environment*, 8, 127-150. Recovered from https://doi.org/10.1016/0034-4257(79)90013-0

Verstraete, M. M., & Pinty, B. (1996). Designing optical spectral indexes for remote sensing applications. *IEEE Transactions in Geoscience and Remote Sensing*, 34, 1254-1265. DOI: 10.1109/36.536541

Wright, J. L. (1982). New evapotranspiration crop coefficients Journal of Irrigation and Drainage, 108, 57-74. Recovered from https://eprints.nwisrl.ars.usda.gov/id/eprint/382